Cementitious materials in biogas systems: Biodeterioration mechanisms and kinetics in CEM I and CAC based materials

Célestine Voegel, Marie Giroudon, Alexandra Bertron, Cédric Patapy, Matthieu Peyre Lavigne, Thomas Verdier, Benjamin Erable

Cementitious materials in biogas systems: biodeterioration mechanisms and kinetics in CEM I and CAC based materials

Célestine Voegel[1,2], Marie Giroudon[1,3], Alexandra Bertron[1*], Cédric Patapy[1], Matthieu Peyre Lavigne[3], Thomas Verdier[1], Benjamin Erable[2]

[1] LMDC, Université de Toulouse, INSA, UPS, 135 Avenue de Rangueil, 31077 Toulouse cedex 04 France

*bertron@insa-toulouse.fr, INSA Toulouse Dép. Génie Civil, 135 avenue de Rangueil, 31077 Toulouse Cedex 4

[2] Laboratoire de Génie Chimique, Université de Toulouse, CNRS, INPT, UPS, Toulouse, France

[3] LISBP, Université de Toulouse, CNRS, INRA, INSA, 135 Avenue de Rangueil, 31077 Toulouse cedex 04 France

ABSTRACT

In anaerobic digestion plants, biological activities transform biowaste into a renewable energy: the biogas. This process produces aggressive and complex media in direct contact with the structure. Few studies have focused on the deterioration of concrete in such environments. In order to support the sustainable development of biogas production growing sector, this study intends to provide thorough information on the biowaste chemical composition and on materials biodeterioration mechanisms occurring in biogas plants. Cementitious materials with various surface compositions (pastes of CEM I, CAC and CEM I treated with oxalic acid) were immersed in the liquid phase of laboratory bioreactors reproducing anaerobic digestion conditions. Altered depths measurements in time highlighted the better resistance of the CAC material. The

microbial biofilm coverage on the material's surface was delayed by the surface pretreatment with oxalic acid and was less dense for the CAC paste. Chemical and mineralogical analyses mainly showed leaching and carbonation phenomena.

Keywords: degradation, cement paste, durability, SEM, calcium aluminate cement

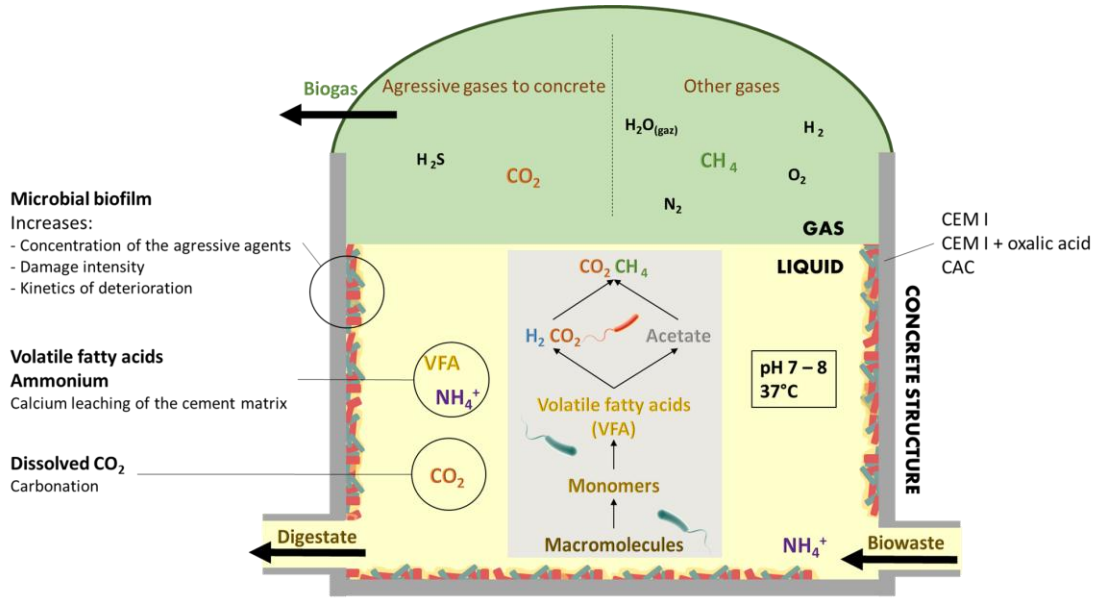

1. INTRODUCTION

The microbial fermentation of organic matter in the absence of oxygen, called anaerobic digestion, leads to the production of biogas, a sustainable fuel gas energy mostly composed of methane (65% CH_4) but also containing a significant amount of carbon dioxide (35% CO_2), and leaves a solid residue, the digestate.

Anaerobic digestion ensures the treatment of biowaste directly at the production source (thus reducing the final quantity of waste). Biogas can be used to produce heat with a good energy efficiency and can also be used as a fuel to produce electricity, with a lower yield. The most common energy recovery method for

biogas is cogeneration, which consists of combining the production of heat and of electricity by recovering the heat of combustion to transform it into electricity [1]. The digestate, made up of non-biodegradable organic matter (mostly lignin is the case of vegetal waste), mineral matter and water, is used as a soil fertilizer and can be a source of additional revenue [2]. In addition, anaerobic digestion permits greenhouse gas emissions to be reduced and helps to increase the incomes of the biogas plants operators. This technology of sustainable energy production has been evaluated as one of the most energy-efficient and environmentally friendly [3].

In view of these multiple advantages, biogas production by anaerobic digestion is strongly encouraged by European policies and its development has become global, using many sources of organic waste. Since 2009, the number of biogas plants in Europe has steadily increased from 6227 to 17662 anaerobic digestion structures in 2016 [4].

As for agricultural and agro-industrial buildings, concrete is the material the most commonly used for the construction of biogas plants. This is related not only to its low cost and ease of implementation but also to its air- and water-tightness and its good thermal inertia [5,6]. However, in digesters, structural concrete is directly in contact with both the liquid and gas phases of the digesting biowaste, which are aggressive to concrete [7,8].

Biogas is the final product of four consecutive degradation reactions that make up the anaerobic process: hydrolysis, acidogenesis, acetogenesis and methanogenesis [9,10]. In most plants, the digestion process is performed under mesophilic conditions, with an optimal operating temperature of around 37°C which requires low self-consumption of energy for the heating [11]. In the first

66 step of the process, hydrolysis decomposes complex organic polymers (proteins,
67 lipids and carbohydrates) into simple soluble molecules: amino acids, long-chain
68 fatty acids and sugars. These compounds are then reduced into short chain
69 volatile fatty acids (VFA) during the acidogenesis step. Acetogenic bacteria
70 degrade the organic acids into acetate, hydrogen and carbon dioxide. These
71 three compounds are finally consumed by the methanogenic archaea to produce
72 methane, and also CO_2 [12–14]. The degradation of nitrogenous compounds
73 such as proteins and urea leads to the production of ammonia, mainly present in
74 the form of ammonium ions under the pH conditions of the anaerobic digestion
75 [15,16].

76 Consequently, by being in contact with the biowaste at every step of the
77 anaerobic digestion, concrete may undergo deterioration due to both the
78 chemical and biological agents. Several compounds in the medium [6,7] are
79 aggressive to concrete: volatile fatty acids, excreted by the acidogenic bacteria,
80 ammonium and dissolved CO_2:

81 • Volatile fatty acids metabolized during anaerobic digestion are organic
82 acids whose calcium salts are soluble in water. Even if the acidity of
83 organic acids is lower than mineral acids, the buffer effects and the
84 solubility of the organic salts make them not less aggressive to concrete.
85 Their attack results in a progressive dissolution of all the initial hydrated
86 phases of the cement paste [17–19].
87 • The ammonium cation NH_4^+ is the conjugated acid of ammonia NH_3,
88 produced during the anaerobic digestion. The ammonium ion react with
89 the cementitious matrix supposedly according to an exchange mechanism
90 $2\ NH_4^+ \longrightarrow Ca^{2+}$ [20,21]. This leads to the dissolution of portlandite and C-
91 S-H and the decalcification of the cementitious matrix [22,23].

- The presence of carbon dioxide in the medium leads to the carbonation of the cement paste: portlandite and C-S-H are dissolved and calcium carbonates are formed [24–26]. Even if most of the time, carbonation can be beneficial for the concrete durability by clogging the porosity [24,25], in submerged systems such as anaerobic digestion medium, dissolved CO_2 can lead to the dissolution of calcium bearing phases, including the calcium carbonates [21].

The microorganisms involved may organize themselves as a biofilm on the surface of the material [27] and induce very high local concentrations of aggressive agents, accentuating the deterioration [7,28]. In this context, the concrete undergoes deterioration resulting in increased porosity and reduced impermeability, leading to a greater risk of reinforcement corrosion [6,29]. Damage to the structures could lead to both important economic and environmental impacts such recovery of a smaller amount of biogas, pollutant flows nearby the plant, and the need for repairs.

The European standard EN 206 [30] and the French information document FD P 18-011 [31] classify environments that are chemically aggressive for concrete by defining three classes of increasing aggressiveness, XA1 to XA3. Among the aggressive species present in the liquid phase of fermenting biowaste, the texts consider the presence and the concentration of carbon dioxide (aggressive CO_2), sulphate (SO_4^{2-}), magnesium (Mg^{2+}), and ammonium (NH_4^+), together with the pH and the water hardness. However, neither document considers the action of organic acids or of microorganisms [17,29], nor the temperature effect, which could accelerate the degradation reactions [32]. Moreover, the pH is not suitable to characterize the aggressiveness of some liquid media, including those containing organic acids [5,33]. It therefore appears that the normative texts are

incomplete as far classifying the aggressiveness of agricultural environments, and especially the anaerobic digestion environment, is concerned. In order to facilitate their classification in the standards, better knowledge of these complex environments, in terms of composition and aggressiveness toward concrete, is needed.

This study aims to (i) widely characterize the medium in terms of chemical composition; (ii) identify and understand the biodeterioration mechanisms and (iii) compare the performances of different cementitious materials (CEM I, CAC and CEM I surface-treated with oxalic acid). The influence of the oxalic acid treatment, the type of binder and the biofilm coverage on the material durability are discussed.

2. MATERIALS AND METHODS

2.1 Materials

2.1.1 Cement paste manufacturing

Three types of materials were used for this study: (i) cement pastes of ordinary Portland cement, CEM I 52.5 R (denominated CEM I); (ii) cement pastes made of calcium aluminate cement, Secar 51 RG (CAC) (chemical oxide composition and Blaine specific surface of both the previous cements are given in Table 1) and (iii) CEM I pastes the surface of which had been treated with a 0.28M oxalic acid solution (denominated CEM I-Ox) [34]. CEM I paste was considered as the reference material and CAC and CEM I-Ox cements were chosen because of their already proven higher durability in an acid environment [33–36].

Table 1. Oxide compositions of the cements in mass percentages and Blaine's specific surface area

	CaO	SiO_2	Al_2O_3	Fe_2O_3	MgO	SO_3	Na_2O	K_2O	Blaine's specific surface (cm^2/g)
CEM I	64.5	20.1	4.83	2.47	1	3.49	0.14	0.17	4970
CAC	44	5.6	52.9	1.47	0.2	<0.2	0.23	0.37	3870

According to several authors [33,35,36], calcium aluminate cements show high durability in acidic media, with a good chemical stability. This could be explained by the alkalinity and the stability of the initial (e.g. katoite C_3AH_6, aluminium hydroxide AH_3) phases and that newly formed through acidic attack, aluminium hydroxide AH_3, which has a high thermodynamic stability [37,38]. Moreover, the alkalinity of CAC binders vs. OPC ones is detailed in the study of Buvignier et al. [39] by comparing the neutralization capacity of an OPC with the one of CAC-based materials on the basis of the calculation by Letourneux and Scrivener [40]. The higher neutralization capacity of the CAC was highlighted and it was assumed that it could contribute to the higher resistance of CAC materials to microorganisms-bearing environments by hindering or inhibiting microbial activity on their surface [39].

Chemical action of the oxalate anion has already been studied and used to provide a surface protection for marble [41,42]; electron microscope observations showed a structural correspondence between the calcium oxalate and the calcite crystals of the marble [43]. The chemical reaction is thought to be based on the transformation of calcium carbonate from the marble into calcium oxalate [44]. This surface layer protects the marble without clogging the pores of the stone [42]. This type of treatment has also been explored on cementitious materials in

laboratory studies, which have shown that, despite the very low pH of the oxalic solution used (pH=1), ordinary Portland paste does not lose mass and is not degraded in depth [33,34]. Calcium oxalate forms a layer on the surface of the material, filling the peripheral porosity. The salt formation is believed to be due to the reaction of the oxalate solution with the Portland cement matrix [17], where the sacrificial dissolution of the portlandite allows the formation of calcium oxalate in the outer layer of the paste specimen. According to Larreur-Cayol et al. [33], the protective effect of the calcium oxalate salt could come from its molar volume which allows the salt to fill the volume released by the dissolution of portlandite and also some of the capillary porosity. Voegel et al. [34] also showed that the oxalic acid treatment on a CEM I paste could delay the paste alteration by an acetic acid solution.

The CEM I and CAC paste specimens were made with a water/binder ratio of 0.4. This ratio optimizes the effects of the acid oxalic treatment and a study by Voegel et al. [34] showed that the water/binder ratio of 0.4 led to a positive mass variation, whereas no mass change was detected for a ratio of 0.27. Thus, the higher porosity of the matrix with a water/binder ratio of 0.4 could have led to the precipitation of a larger amount of calcium oxalate [34]. The pastes were mixed according to the French standard NF EN 196-3 [45] and cast in cylindrical moulds 75 mm high and 25 mm in diameter. The pastes were cast in three consecutive layers, each vibrated for 120 seconds. They were removed from their moulds 24h after pouring. Then, each specimen underwent an exogenous cure in a small amount of water at 20 °C for 27 days, which allowed the hydration to continue while limiting leaching. After the curing period, 5 mm thick slices were sawn from paste cylinder specimen, to be used for the biofilm growth testing. Also, some CEM I paste cylinders and slices were immersed in a 0.28 M oxalic acid solution

188 ($C_2H_2O_4$) (pH=0.76) for 7 days, the other specimens being kept in sealed bags.
189 The initial porosities of the paste specimens were measured by water intrusion
190 porosimetry adapting the French standard NF P18-459 [46] for cement pastes
191 specimens. The results were 40±1 % for CEM I and 27±1 % for CAC.

192 *2.1.2 Characterization of cement paste surfaces*

193 Just before immersion in the biowaste, the surface pH of the specimens was
194 measured with pH paper: it was between 12 and 13 for the CEM I and CAC
195 pastes (sound cementitious materials) whereas it was about 1 for the CEM I-Ox
196 paste (because of the pH 0.76 oxalic acid treatment) [27].

197 The main mineralogical phases of the cement pastes surfaces before the
198 immersion were determined by X-Ray Diffraction (XRD) analyses. The
199 diffractograms showed the phases habitually encountered in sound CEM I and
200 CAC cement pastes. The CEM I paste surface was composed of C-S-H,
201 portlandite ($Ca(OH)_2$), ettringite, C_xAH_y, C_3S and C_2S. The CAC paste surface
202 showed C_3AH_6, gibbsite (AH_3), gehlenite (C_2AS), mayenite ($C_{12}A_7$), C_2AH_8,
203 brownmillerite (C_4AF) and calcium aluminate oxide (CA). Microscopic
204 observations (performed with a Scanning Electron Microscope (SEM) in back
205 scattered electron mode (BSE)) and mineralogical analysis (by XRD) were made
206 on the surface of the CEM I specimens treated with oxalic acid. They showed an
207 adherent, continuous layer of precipitate of whewellite (calcium oxalate
208 monohydrate) covering the whole specimen (Figure 1). This layer was formed
209 over a thickness of 100 to 200 µm and clogged the porosity locally [33,34]. More
210 details about the method are given in §2.5.

211

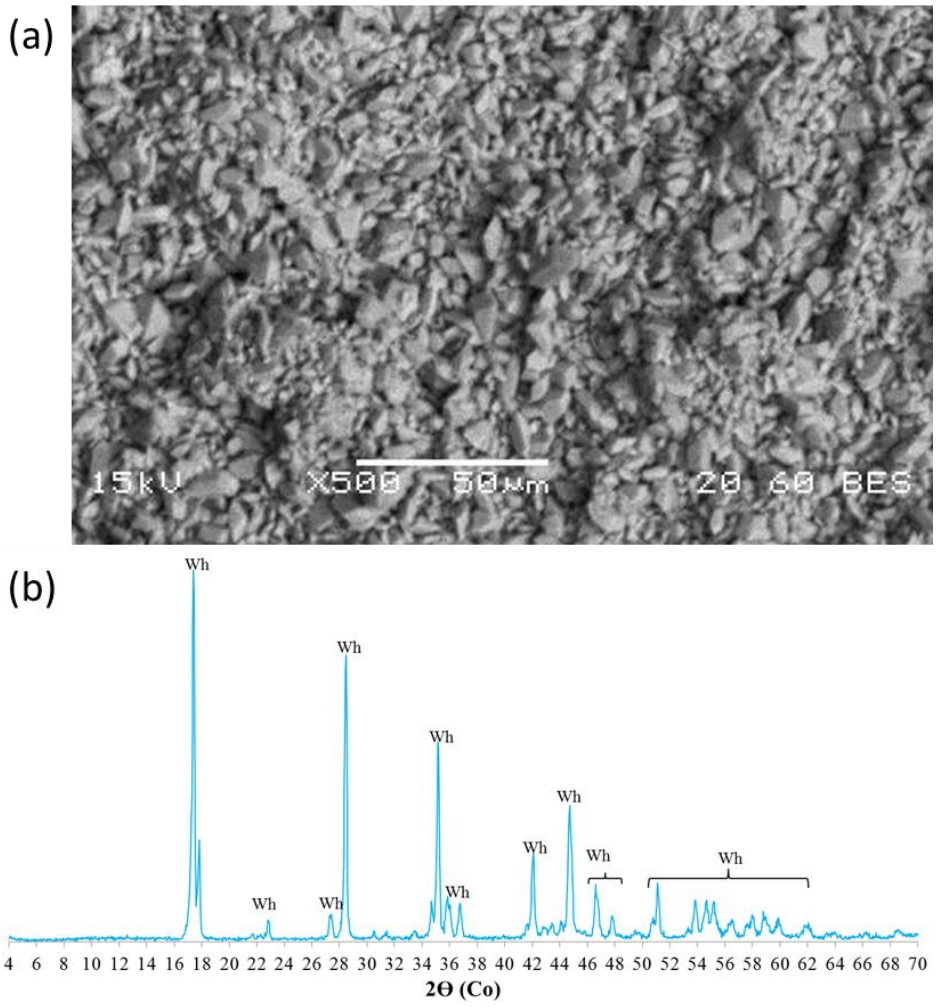

Figure 1. (a) SEM observation and (b) mineralogical analysis of the CEM I-Ox paste surface after the 7 days oxalic acid treatment (Wh: whewellite (calcium oxalate monohydrate))

2.2 Immersion of cement pastes in the synthetic biowaste

The substrate for biogas production by anaerobic digestion used in this study was a laboratory synthetic biowaste representative of the organic domestic waste currently produced in France according to the CIRSEE (International Research Center On Water and Environment). Its composition was provided by IRSTEA of Antony (France): a mix of different food products. All the details on composition and production are given in Voegel et al. [7]. Bacterial inoculation was made from a sludge sampled in a municipal wastewater treatment in Toulouse (France) in

224 order to induce the anaerobic digestion process [47]. The inoculation was
225 operated with a $V_{inoculum}/V_{substrate}$ ratio of 2.5, which corresponded to an optimal
226 ratio of 1 g $COD_{inoculum}$/ g $COD_{substrate}$,(with COD the chemical oxygen demand) as
227 already established in previous works [7,48]. Cement pastes were totally
228 immersed in the liquid phase of the biowaste in anaerobic bioreactors for 5
229 weeks. The surface area/volume ratio (cement paste surface area/inoculated
230 biowaste volume) was 224 cm^2 L^{-1} for the cylindrical samples and 34 cm^2 L^{-1} for
231 the slices used for biofilm development monitoring. These two ratios are quite
232 high in comparison with real situations of industrial digester (4 cm^2 L^{-1} [48]) but
233 allow to amplify the phenomena occurring close to the material. The bioreactors
234 (two reactors per type of material, experiments run in duplicate) were kept in an
235 oven at 37° C throughout the experiment. The reaction medium, with an initial
236 volume of 525 mL, was continuously stirred by a magnetic stirring system.
237 Biowaste was renewed at the end of each 5-week digestion cycle. This period
238 corresponds to the average time required for the complete digestion of a
239 substrate [49] and is commonly used as a typical duration for laboratory tests
240 [50,51]. Two cycles were carried out.

241 **2.3 Analysis of the liquid phase of the digesting biowaste**

242 The liquid phase composition of the digesting biowaste was monitored over time
243 in order to analyse the concentration of organic acids, ammonium and CO_2, and
244 the pH [7]. Regular sampling of 1.5 mL of the liquid phase was carried out and
245 concentrations of the organic acids were measured using High Performance
246 Liquid Chromatography analyses (Thermo Fisher U3000; column: Aminex HPX-
247 87H BIORAD; eluant: H_2SO_4; flow rate: 0.5 $mL.min^{-1}$) [7,48]. Ammonium
248 concentrations were measured using Ionic Chromatography (Thermo Electron
249 ICS 3000, column: CS16; pre-column; cartridge holder; eluant: 30 mM

methanesulfonic acid; flow rate: 1.0 mL.min^{-1}). The soluble CO_2 produced from the microbial activity was occasionally determined by analysis of total inorganic carbon (TOC-SCHIMADZU) [7].

2.4 Observation of biofilm on cement pastes

Cement paste slices were sawn carefully in order to preserve the biofilm on their surfaces. Before the observations, the biofilms were first chemically fixed and then dehydrated according to the method of Voegel et al. [7,48]. The biofilm was observed by SEM-FEG (JEOL 7100F TTLS combined with EDX XMax, 5kW) after 5 weeks (CEM I, CEM I-Ox, CAC) and 10 weeks (CEM I-Ox).

2.5 Microscopic observations and analysis of chemical and mineralogical changes in cementitious materials

The cylindrical cement paste specimens were removed from the biowaste after each digestion cycle (i.e. after 5 and 10 weeks of immersion) and 5 mm cement paste slices were collected by sawing the cylindrical specimens perpendicularly to their longitudinal axis with a diamond saw. A part of a slice was then embedded in an epoxy resin (Mecaprex MA2+ by Presi) and dry-polished using silicon carbide polishing disks (Presi) according to the procedure described by Bertron et al. [52]. The polished sections were coated with carbon before being analysed. Microstructural observations of cement pastes were made by Scanning Electron Microscopy (SEM, JEOL JSM 6380LV) using back scattered electron (BSE) mode. Chemical analyses were performed on the same specimens using energy dispersive X-ray spectrometry (EDS, Brucker Xflash 6/30 - SDD) and electron-probe micro-analysis (EPMA, Cameca SXFive, 15 kV, 20 nA, scanning area of the beam 2 x 2 µm^2). Punctual analyses were carried out by positioning a hundred points manually, carefully avoiding anhydrous grains, from the degraded

surface to the sound core [7]. A microstructural and chemical zonation of the deteriorated specimens according to the distance to the surface was identified from the correlated results of SEM+EDS and EPMA: the zonation is primarily set through chemical composition profiles obtained from EPMA and then X-ray diffraction (XRD) analyses are performed to evaluate the mineralogical composition in each zone. Mineralogical analyses in the different zones identified were carried out by XRD (Siemens D5000, Co cathode, 40 kV, 30 nA) using the procedure presented in Bertron et al. [53].

3. RESULTS

3.1 Composition of the liquid fraction of the digesting biowaste

Table 2 summarizes the composition of the liquid fraction of the bioreactors through several cycles. The values in the table are averages over the six bioreactors run at the same time (two bioreactors per material type). Figure 2 shows the typical evolutions of the pH and the acid concentrations during a cycle of anaerobic digestion [7].

From Table 2, no major difference in the composition of the liquid fraction is observed between the two cycles (5 and 10 weeks). The acetic acid concentration reaches 23 $mmol.L^{-1}$ on average, whereas the propionic and butyric acids concentrations reach 9 $mmol.L^{-1}$. Table 2 and Figure 2 show that the pH decreases in the first few days, to values around 4.5. Within this period, hydrolysis and acidogenesis steps correlated with the production of organic acids. After that, the pH reaches 7.0 on the 10^{th} day and stabilizes around 7.8 thereafter due to a progressive and then total consumption of the VFA during the acetogenesis and methanogenesis steps. Koenig and Dehn [8] found similar pH values (pH of approximately 7) in the liquid phase of their laboratory fermenter.

The average ammonium concentrations reach 55 mmol.L^{-1}. This value is consistent with the studies by Voegel et al. [7] and Giroudon et al. [54], where the evolutions of the ammonium concentration were similar and reached about 800 mg.L^{-1} (40 mmol.L^{-1}) and with McCarty [49] who states that ammonium concentrations can reach 1000 mg.L^{-1} for a digester in good function.

Punctual analyses of dissolved CO_2 concentrations showed that, after 3 weeks of biowaste anaerobic digestion, the CO_2 concentration was 2.3 mmol L^{-1} ± 0.2 mg.L^{-1}. The digesting biowaste contained little or no sulfur bearing compounds.

Table 2. Composition of the liquid fraction of the digesting biowaste in terms of VFA concentration, ammonium concentration and pH: minimum value–maximum value (standard deviations).

	VFA concentration (mmol.L^{-1})			Ammonium concentration (mmol.L^{-1})	pH
	Acetic acid	Propionic acid	Butyric acid		
1st cycle (week 1 to 5)	0.14-22.99 (0.22-2.14)	0.26-10.79 (0.12-2.54)	0.00-8.31 (0-1.17)	0.85-54.90 (0.11-1.00)	4.33-7.81 (0.31-0.18)
2nd cycle (week 6 to 10)	1.14-24.42 (0.10-2.87)	0.14-9.84 (0.09-2.55)	0.00-9.83 (0-2.32)	0.83-52.24 (0.09-2.11)	4.47-7.52 (0.23-0.15)

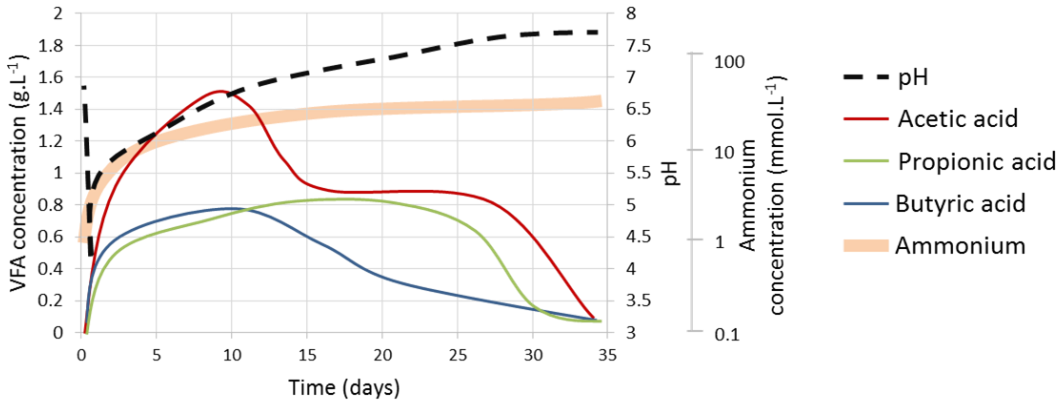

Figure 2. Typical evolution of pH, VFA concentrations and ammonium concentration for a single anaerobic digestion cycle, adapted from Voegel et al. [7]

3.2 Altered depths of the cement pastes

Figure 3 shows the altered depths of the cement pastes after 5 weeks (one digestion cycle) and 10 weeks (two digestion cycles) of immersion in the digesting biowaste. Altered depths were obtained by analyses of flat polished sections using BSE-mode SEM coupled to EDS and EPMA. Altered depths correspond to limits between the sound zone (zone 1) and the beginning of the altered zone (zone 2) on Figures 5, 7 and 9.

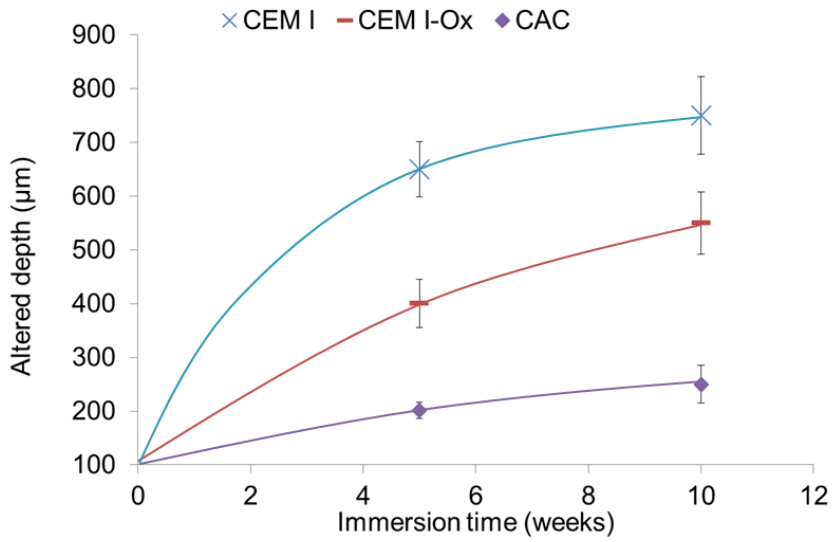

Figure 3. Altered depths of the cement pastes immersed in the digesting biowaste

After 5 weeks of exposure to the digesting biowaste, the CAC samples had the smallest altered depth (200 µm) whereas CEM I-Ox and CEM I pastes had altered depths of 400 and 650 µm respectively. After 10 weeks, the degraded depth of the CAC pastes had increased slightly, reaching a value of 250 µm, whereas CEM I-Ox and CEM I reached degraded depths of 550 and 750 µm.

During the first cycle (< 5 weeks), the protective properties of the calcium oxalate seemed to be efficient as the CEM I-Ox degraded depth was 1.6 times less than that of CEM I pastes. During the second cycle (between 5 and 10 weeks), the

increase of the degraded depth of the CEM I-Ox paste was 150 µm which was greater than the increase of the degraded depth of the non-treated CEM I paste (of 100 µm). Thus, it seems that the calcium oxalate treatment was no longer effective at this point.

The CAC pastes showed positive achievement throughout the experiment as their degraded depths after 10 weeks were only 250 µm which was 2 or 3 times less than the CEM I-Ox and CEM I degraded depths after 5 weeks.

3.3 Microscopic observation of biofilms

Figure 4 presents the SEM observation of the surface of CEM I, CAC and CEM I-Ox pastes after 5 weeks of immersion and 10 weeks of immersion for the CEM I-Ox sample. At both sampling dates (i.e. 5 and 10 weeks), the CEM I pastes surfaces showed a uniform, dense biofilm whereas the biofilm observed on the surface of the CAC was less dense, with few microorganisms. In contrast, microbial colonization was not observed on the surface of the CEM I-Ox slice after 5 weeks of anaerobic digestion and calcium oxalate precipitates, similar to those observed on the cement paste immediately after the oxalic acid treatment (Figure 1), covered the surface. After 10 weeks of immersion, the entire surface of the CEM I-Ox paste was covered by a dense biofilm and calcium oxalate precipitates were no longer observed. It can be assumed that between 5 and 10 weeks of exposure the surface conditions enabled a biofilm to form on the surface. The biofilm may have produced local conditions that finally dissolved the oxalate salt.

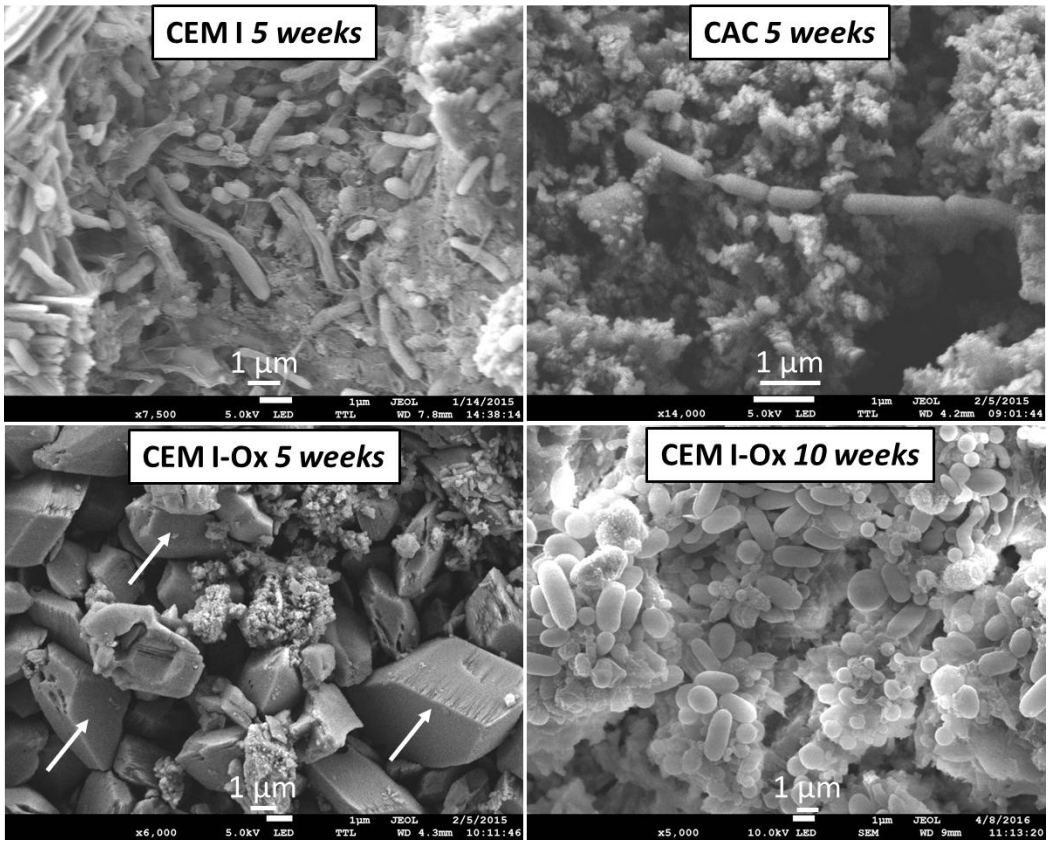

357

358 **Figure 4. SEM observations of biofilms on cement pastes after 5 weeks**
359 **(CEM I, CAC, CEM I-Ox) and 10 weeks (CEM I-Ox) of immersion in the**
360 **digesting biowaste. Calcium oxalate crystals are identified by white arrows.**

361 **3.4 Chemical and mineralogical analysis of the cementitious specimens**

362 *3.4.1 CEM I paste*

363 The chemical composition profiles of the CEM I paste sample at 10 weeks of
364 immersion, as a function of the distance to the surface, and the image of the
365 same specimen by SEM in back-scattered electron (BSE) mode are presented on
366 the right side of Figure 5. The outer layer of the specimen was partly dissolved
367 when it was removed from the biowaste. The thickness of the material lost is
368 reported on the figure (about 150 µm) and was measured by measuring the
369 difference between the initial diameter of the sample and its final dimensions. The
370 left side of Figure 5 gives the chemical composition profile of the outer layers of
371 the CEM I paste immersed for 5 weeks in the fermenting biowaste (adapted from

Voegel et al. [7]). A chemical zonation of the specimens was identified and is represented on the figure, from zone 1, corresponding the intact core, to zone 5, corresponding to the outer layer in contact with the biofilm and the biowaste. The mineralogical characterization by XRD in each zone defined in Figure 5 is presented in Figure 6. From the core to the outer layer, the chemical and mineralogical evolution of the cementitious matrix is as follows:

- Zone 1 corresponds to the sound zone. The mineralogical analyses showed a composition similar to that of an unaltered specimen, mainly made of hydrated phases (portlandite, ettringite, and C-S-H) and anhydrous grains (C_3S, C_2S, brownmillerite C_4AF). The SEM observations show the high density of the anhydrous residual cement grains (in lighter grey on the SEM image).
- Zone 2 is 350 µm thick and shows the same two main phenomena in each cycle: (i) a slight decalcification corresponding to the dissolution of portlandite, and (ii) an enrichment in sulfur, which can be correlated with a slight intensification of the ettringite peaks in the mineralogical pattern (Figure 6). This secondary ettringite comes from the diffusion of sulfates from the altered zone, and is classically observed in transition zone of specimens exposed to leaching [53,55]. It is probably not expansive as no microcracks are observed by SEM in this zone. The density of the anhydrous grains remains high in this zone, as can be observed in the SEM picture.
- After each cycle, zone 3 is mainly characterized by the dissolution of the anhydrous grains shown in the SEM picture and a lower density of the hydrated matrix (darker colour of the cement paste). The mineralogical pattern (Figure 6) shows that calcite is the main crystallized phase in this

zone and that ettringite, C_3S, C_2S and brownmillerite phases are dissolved. The chemical composition (Figure 5) shows the decrease in the sulfur content, correlated with the disappearance of the ettringite peaks and the decrease of the total amount of oxides. This zone is 180 µm thick.

- Zone 4 is mainly composed of the two polymorphs of calcium carbonate ($CaCO_3$), calcite and vaterite, which form for C/S ratio ≥ 0.67 in the C-S-H [56]. The chemical composition (Figure 5) shows the partial decalcification of the sample and a peak of phosphorous, probably brought by the biowaste. No peak of a crystallized phase containing phosphorus is visible on the diffraction pattern, at either 5 or 10 weeks, suggesting that an amorphous P-phase has precipitated. This zone is 30 µm and 80 µm thick respectively after the 5^{th} and the 10^{th} weeks, respectively, and shows a low density in the SEM image.
- Zone 5 is the outer layer, mainly visible after 5 weeks (70 µm thick). This zone is mainly amorphous (Figure 6) and is likely to be composed of a Si-Al gel, containing phosphorus in its outer part. At 10 weeks, it can be assumed that this external zone was partially dissolved or detached from the matrix. The missing zone was determined to be around 150 µm thick according to image analysis measurements performed on the cross section of the specimen.

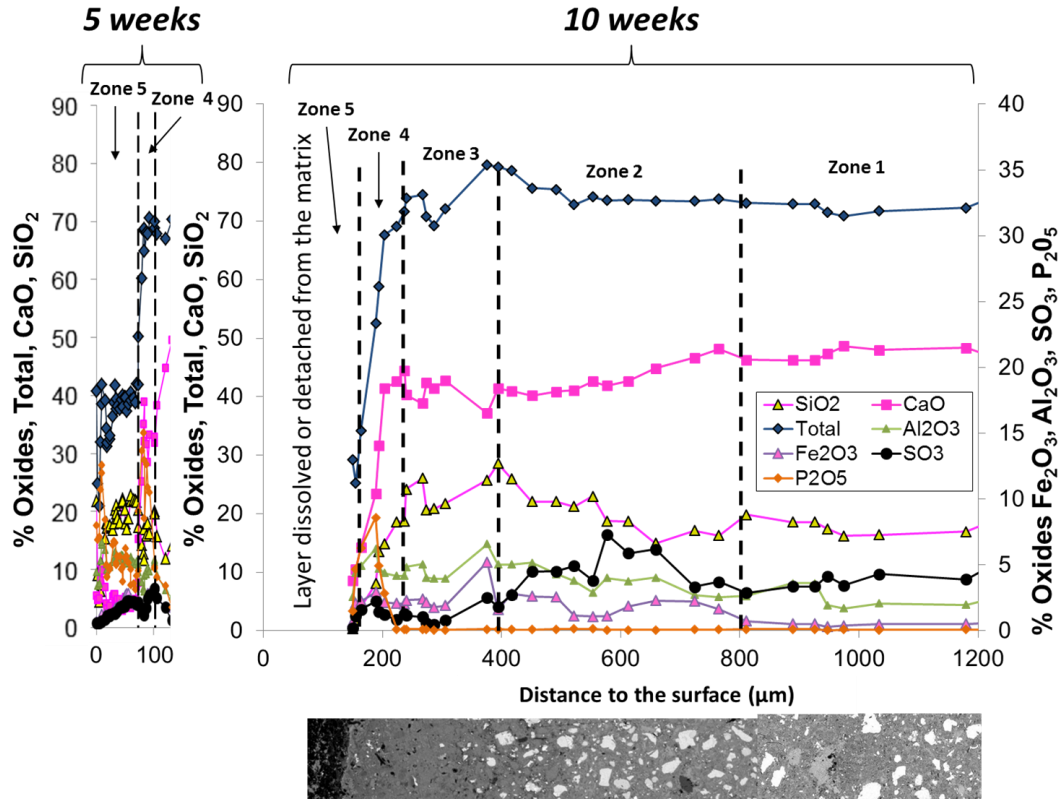

418

419 **Figure 5. Chemical composition after 10 weeks of immersion and chemical**
420 **composition of the outer layers of the CEM I paste after 5 weeks [7]**
421 **according to the distance to the surface (EPMA) (top) and SEM**
422 **observations of the polished section in BSE mode (bottom)**

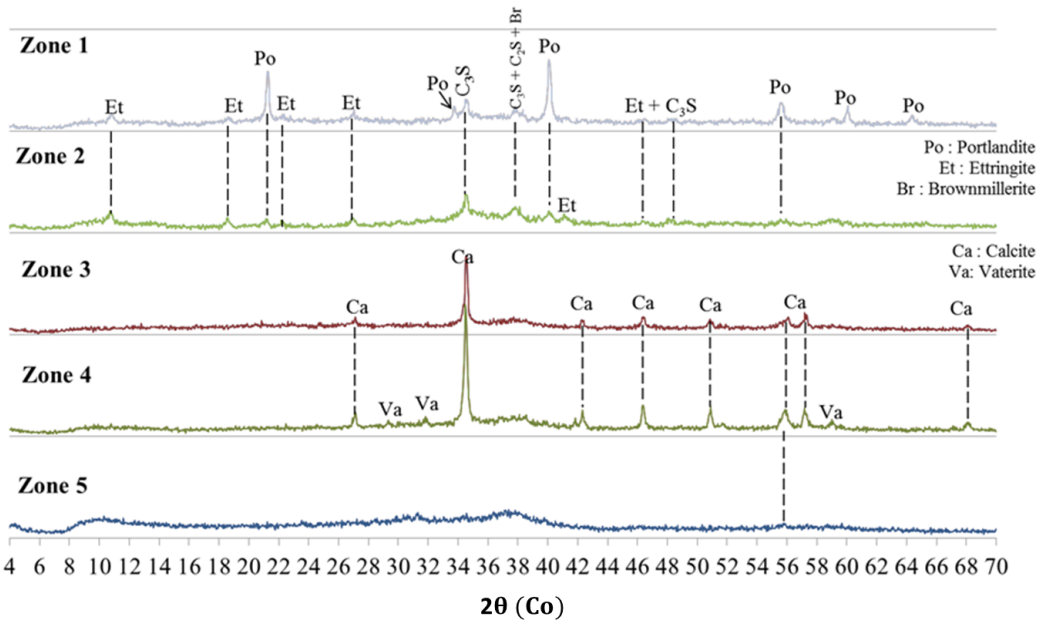

Figure 6. Mineralogical analysis by XRD of CEM I paste immersed for 5 and 10 weeks

3.4.2 CEM I-Ox paste

The chemical composition profiles, according to the distance to the surface, of the CEM I-Ox paste sample at 10 weeks of immersion, and the image of the same specimen by SEM in BSE mode are presented in Figure 7, right side. The left side of the figure gives the chemical composition profile of the outer layers of the CEM I-Ox paste immersed for 5 weeks in the fermenting biowaste. The mineralogical characterization by XRD of each zone is presented in Figure 8. In light of the chemical and mineralogical analyses, four zones can be distinguished after 5 and 10 weeks, with differences in the composition of the outer layer between the two exposure times. The zonation is as follows:

- Zone 1 corresponds to the unaltered zone. Its mineralogical and chemical composition is similar to that of zone 1 of the CEM I paste.
- As for the CEM I paste specimen, Zone 2 shows a slight decalcification with an increase of the sulfur oxide content. From a mineralogical point

of view, portlandite peaks are reduced whereas ettringite peaks are intensified, which could be correlated with the increase of sulfur oxides content. This zone is 400 µm thick and the SEM image shows a less dense structure here than in zone 1.

- Zone 3, 180 µm thick, contains mainly calcium in the form of calcite and vaterite. Anhydrous grains are no longer observed in the SEM image and the paste density has decreased.
- For zone 4, two different patterns are observed at 5 and 10 weeks of exposure to the biowaste. At 5 weeks, this zone is mainly composed of calcium and phosphorus. The CaO content is related to the precipitation of the calcium oxalate salt (whewellite), preserved on the surface, the XRD pattern being very similar to that of the surface before the immersion (Figure 1). The phosphorus enrichment is probably due to diffusion and fixation of this element from the biowaste. At 10 weeks, the calcium content tends to zero in the outer part of this zone. Whewellite has been dissolved and the XRD diffractogram shows an amorphous pattern of the remaining cement matrix.

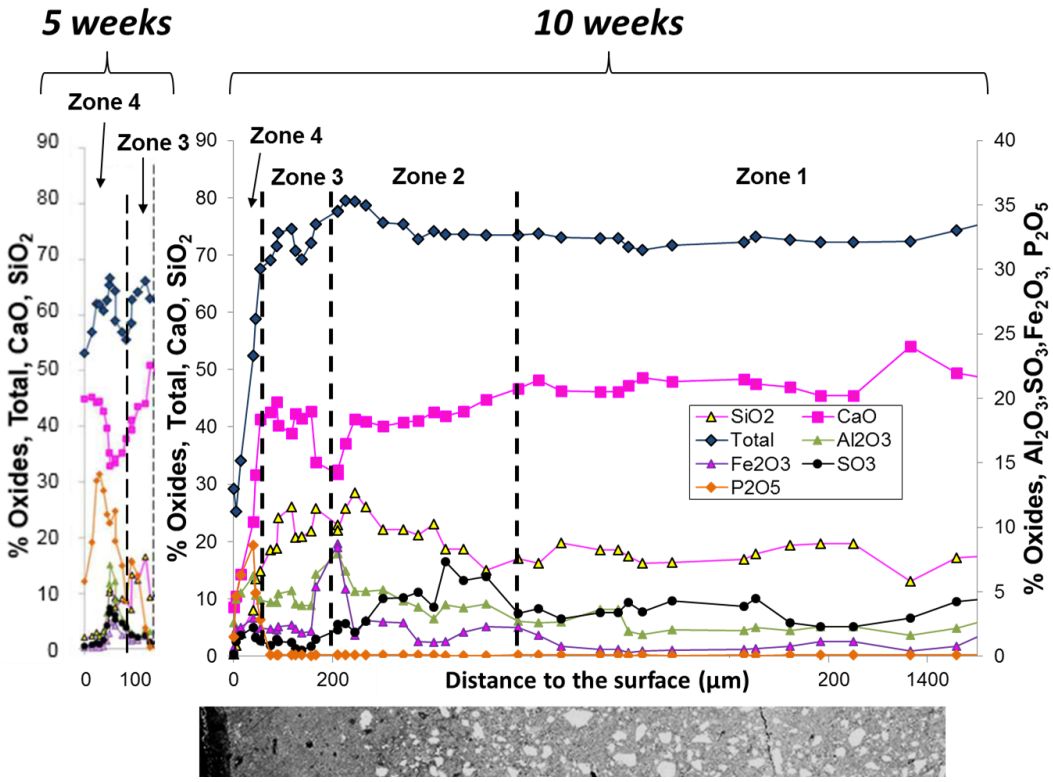

457

458 **Figure 7. Chemical composition of the CEM I-Ox paste after 10 weeks of**
459 **immersion and chemical composition of the outer layers of this paste after**
460 **5 weeks of immersion according to the distance to the surface (EPMA)**
461 **(top), and SEM observations of the polished section in BSE mode (bottom)**

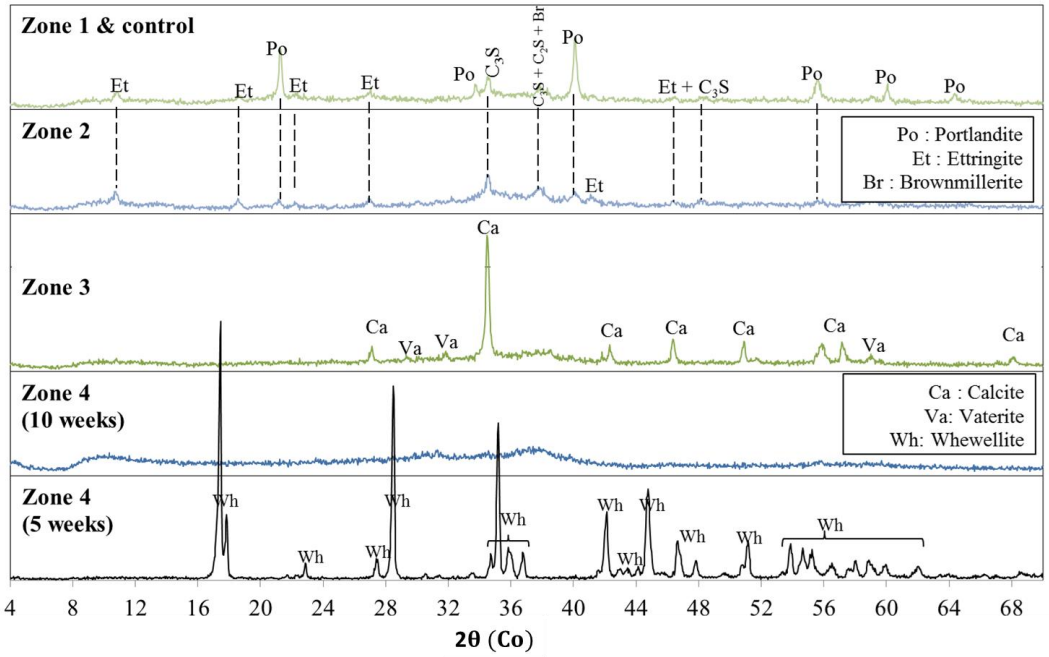

462

463 **Figure 8. Mineralogical analysis by XRD of the CEM I-Ox paste immersed**
464 **for 10 weeks and 5 weeks (Zone 4)**

465 *3.4.3 CAC paste*

466 The chemical composition of the CAC paste after 10 weeks of immersion is
467 presented in Figure 9, together with a BSE-mode SEM image of the sample.
468 Chemical compositions are similar after 5 and 10 weeks. The mineralogical
469 analyses from the core to the surface are presented in Figure 10. Three zones
470 are distinguished:

471 • Zone 1 has similar composition to that of a sound specimen, i.e. it is
472 mainly made of aluminium and calcium, and contains crystalline
473 anhydrous (calcium aluminium oxides (CA), mayenite ($C_{12}A_7$),
474 brownmillerite (C_4AF), gehlenite (C_2AS)) and hydrated phases (C_3AH_6,
475 gibbsite (AH_3), C_2AH_8), usually found in aluminate cement matrices. It
476 shows a high density (lighter grey zone on the SEM images).

- Zone 2, 180 µm thick, shows a slight decalcification, and therefore a slight relative enrichment of Al. Mineralogical analyses show the same phases as in zone 1 overall. However, some slight differences can be noted: the peaks of the anhydrous phases, CA and gehlenite are less intense closer to the surface; in contrast, gibbsite peaks (AH_3) increased. Aragonite is detected, probably due to the carbonation of katoite C_3AH_6 [57]. Moreover, the density of the paste decreases (darker background on the SEM image).
- Zone 3 shows an enrichment in phosphorus with an intense decalcification and a decrease of the aluminium content. However, no peak of a crystallized P-bearing phase is observed on the diffraction pattern. The total oxides content decreases from 65 to 50%. The mineralogical analysis shows intense peaks of AH_3, the broad bases of which characterize the poorly crystallized character of this phase. The density of the peripheral zone remains relatively high.

492

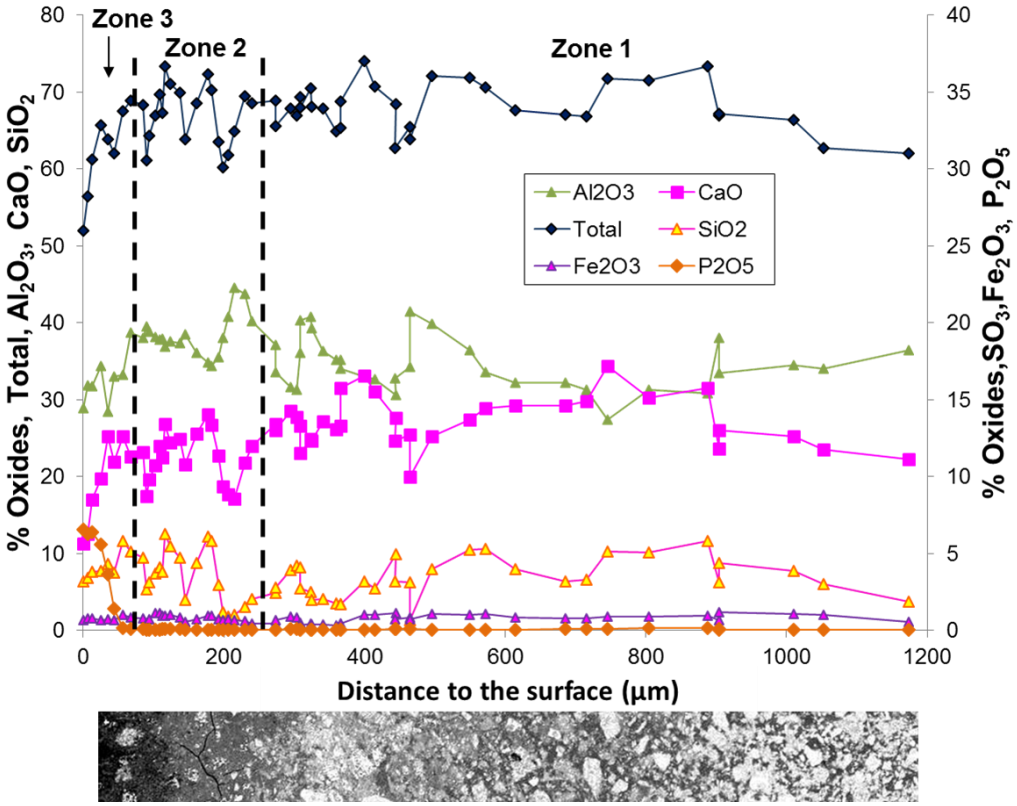

493 **Figure 9. Chemical composition of the CAC paste after 10 weeks of**
494 **immersion according to the distance to the surface (EPMA) (top), and SEM**
495 **observations of the polished section in BSE mode (bottom)**

496

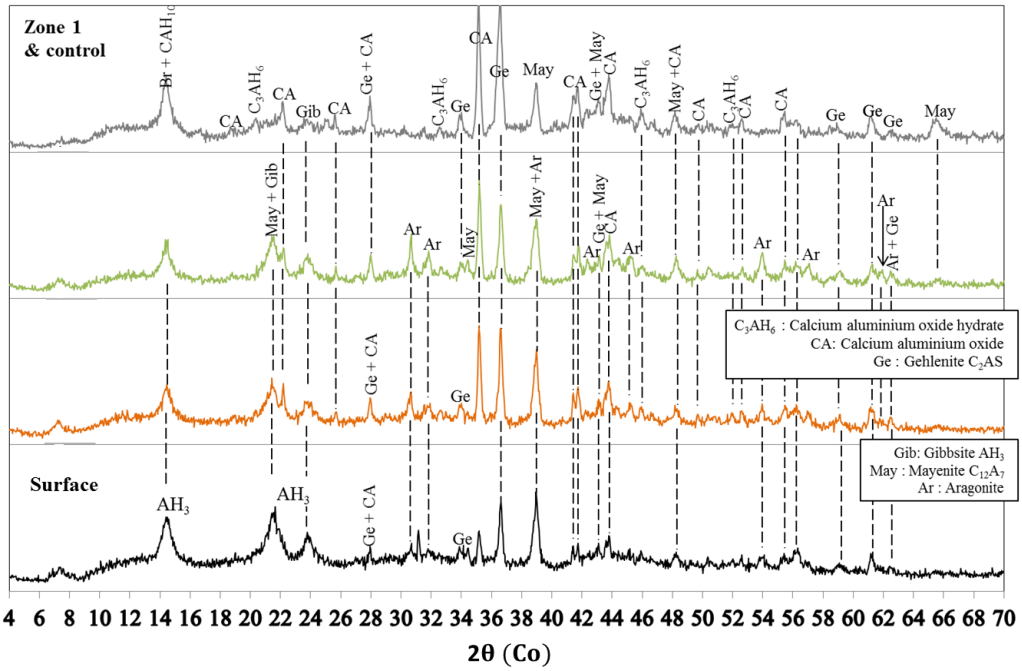

497

498 **Figure 10. Mineralogical analysis by XRD of the CAC paste immersed for 5**
499 **weeks in digesting biowaste**

500

501 4. DISCUSSION

502 **4.1 Chemical and microbial composition of the liquid fraction of the**
503 **digesting biowaste**

504 The liquid fraction contained in lab-scale anaerobic bioreactor has properly
505 undergone the consecutive reactions of the anaerobic digestion process. First,
506 the hydrolysis and acetogenesis steps led to a decrease of the pH and an
507 increase of the VFAs concentration: the total VFAs concentration reached about
508 75 mmol.L^{-1} and the pH dropped to 4.3. The VFAs metabolized in the digesting
509 biowaste were acetic, propionic and butyric acids, which are acids with soluble
510 calcium salts. Then, the acetogenesis and methanogenesis steps gave rise to
511 consumption of the VFAs and an increase to the neutrality area of the pH, which
512 reached 7.8 at the end of the digestion cycle. The ammonium concentration

513 increased quickly during the first few days of digestion and then stabilized at
514 values around 55 mmol.L^{-1}. Both cycles showed similar aggressive conditions in
515 terms of concentrations of aggressive metabolites (VFA, ammonium and
516 dissolved CO_2) and pH values. This means that concrete structures in which
517 anaerobic digestion takes place will undergo repeated aggression when they are
518 replenished in fed-batch, or a continuous aggression in the case of continuously-
519 fed digesting installation.

520 These concentrations of aggressive metabolites in the liquid phase of the
521 bioreactors give information on the aggressiveness of the environment for
522 concrete. Table 3 summarizes the limit values for solutions according to the
523 exposure classes as given in FD P 18-011 [31] for the concentrations of
524 aggressive CO_2 and the ammonium, together with the pH. Considering that, for
525 each cycle, the pH increased to values up to 6.5 after 7 days, the pH of the
526 anaerobic digestion in normal operation should not lead to aggressive conditions
527 for concrete according to the French information document FD P 18-011 [31]
528 where the upper limit of pH of the XA1 exposure class is 6.5. The standard
529 documents [30,31] also take the presence and the concentration of ammonium
530 and dissolved CO_2 into account. The maximum concentration values measured
531 during the anaerobic digestion (55 mmol.L^{-1} for ammonium and 2.3 mmol.L^{-1} for
532 dissolved CO_2) made the liquid phase of the anaerobic digestion a highly
533 aggressive medium for cement based materials (class XA3 according to Table 3):
534 the maximum concentration of ammonium measured was more than 7 times the
535 upper limit considered in the XA3 range (3.33 – 5.55 mmol.L^{-1}) and the dissolved
536 CO_2 concentration was above the lower limit of the XA3 class (1.67 mmol.L^{-1}). It
537 also can be noticed that ammonium and bicarbonate concentrations of several
538 grams per liter have been found in fully functioning industrial digesters [58–60].

539 Moreover, it can be highlighted that neither document considers the presence
540 and concentration of VFA, even though several authors [17,33] have shown that
541 the acid concentration is a much more significant parameter than the pH in the
542 evaluation of the aggressiveness of certain types of acids, including organic
543 acids.

544 The presence and impact of microorganisms, in the form of a biofilm or not, are
545 not considered either by the FD P18-011 [31] regulation. However, the
546 establishment of a microbial biofilm between the 5^{th} and the 10^{th} week was clearly
547 a factor increasing the deterioration kinetics of the CEM I-Ox paste. In contrast,
548 the CAC paste was particularly resilient to the biofilm proliferation and was the
549 material that showed the strongest resistance against the biodeterioration.
550 Several studies agree that microorganisms are acting as accelerating agents on
551 the deterioration of concrete, aggravating its biodeterioration [7,8,28,29,61]. More
552 particularly, a study by Magniont et al. [28] has highlighted the clear influence of a
553 biofilm formation of *E. coli* intensifying the CEM I degradation. In addition, it was
554 also demonstrated that the ability of bacteria to create a biofilm could be very
555 harmful for concrete structures [5,28]. According to the non-aggressive pH-
556 conditions, the dissolution of the external zone (Si-Al gel) of the CEM I paste
557 presently observed after 10 weeks of exposure can be explained by particularly
558 severe local conditions brought by the establishment of a biofilm at the surface.

559 Lastly, the standard considers temperatures between 5 and 25 °C while the
560 anaerobic digestion process occurs mostly at mesophilic conditions (around 37
561 °C) in the industrial sector [11]. Even if a rise in temperature increases reaction
562 rates and finally the concrete degradation kinetics, this factor is not taken in
563 account for the exposure classes.

564 **Table 3. Limit values for exposure classes for liquid environments**
565 **according to FD P 18-011 [31]**

Aggressive agents	Aggressiveness class according to NF EN 206 [30]			In the biowaste studied
	XA1	XA2	XA3	
Aggressive CO_2 ($mg.L^{-1}$)	≥ 15 and ≤ 20	> 40 and ≤ 100	> 100	101
NH_4^+ ($mg.L^{-1}$)	≥ 15 and ≤ 30	> 30 and ≤ 60	> 60 and ≤ 100	990
pH	≤ 6,5 and ≥ 5,5	< 5,5 and ≥ 4,5	< 4,5 and ≥ 4,0	7.5

566

567 **4.2 Performances of tested materials in relation with biofilm-materials**
568 **interaction phenomena**

569 The CEM I paste showed the highest deterioration kinetics, with the greatest
570 degraded depths after 5 and 10 weeks and complete biofilm coverage observed
571 at 5 weeks of exposure. The early microbial colonization of the CEM I paste could
572 be explained by the topology of the surface of CEM I, especially the abundance
573 of micrometric holes, which Voegel et al. [27] found to be favourable to adhesion
574 and microbial proliferation.

575 The oxalic acid treatment has resulted after 5 weeks in a less intense degraded
576 depth than in the CEM I specimen, a chemical composition close to that of a
577 sound sample, and no biofilm coverage. This resistance against the microbial
578 biofilm growth could come from the surface texture created on the CEM I treated
579 by oxalic acid: according to Voegel et al. [27], considering the characteristics of
580 its surface height distribution, the CEM I-Ox paste covered by calcium oxalate
581 was less favourable to microbial growth. However, after 10 weeks of immersion,
582 the salt was no longer observed and the sample was covered by biofilm. The
583 CEM I-Ox paste then showed the same degradation mechanisms as the CEM I

584 paste, with a large degraded depth. Thus, the treatment seemed to have a
585 protective effect for a limited duration only: it allowed degradation to be delayed
586 by delaying the biofilm formation on the surface, which underlines the worsening
587 effect of this formation. The oxalic acid surface treatment probably provided two
588 types of protection: the delay of biofilm formation and the presence of a layer of
589 calcium oxalate, which was initially stable against acid attacks, thus protecting
590 the matrix, but dissolved in the short term, revealing a surface composition close
591 to that of the non-treated CEM I favourable to microbial proliferation.

592 Although the CAC pastes presented surfaces favourable to proliferation [27], this
593 material showed the highest durability, with the smallest degraded depths after
594 10 weeks and only a non-uniform weak surface coverage by a microbial biofilm.
595 The anhydrous phases of the CAC paste were the most preserved and the
596 aluminate cement showed some peaks of crystallized AH_3. However, a halo
597 baseline characteristics of amorphous compounds is also observed on the
598 surface layer.

599 **4.3 Biodeterioration mechanisms**

600 Figure 11 summarizes the main chemical and mineralogical changes in the CEM
601 I and CAC pastes exposed to the anaerobic digesting biowaste for two cycles,
602 together with exposure conditions and degraded depths.

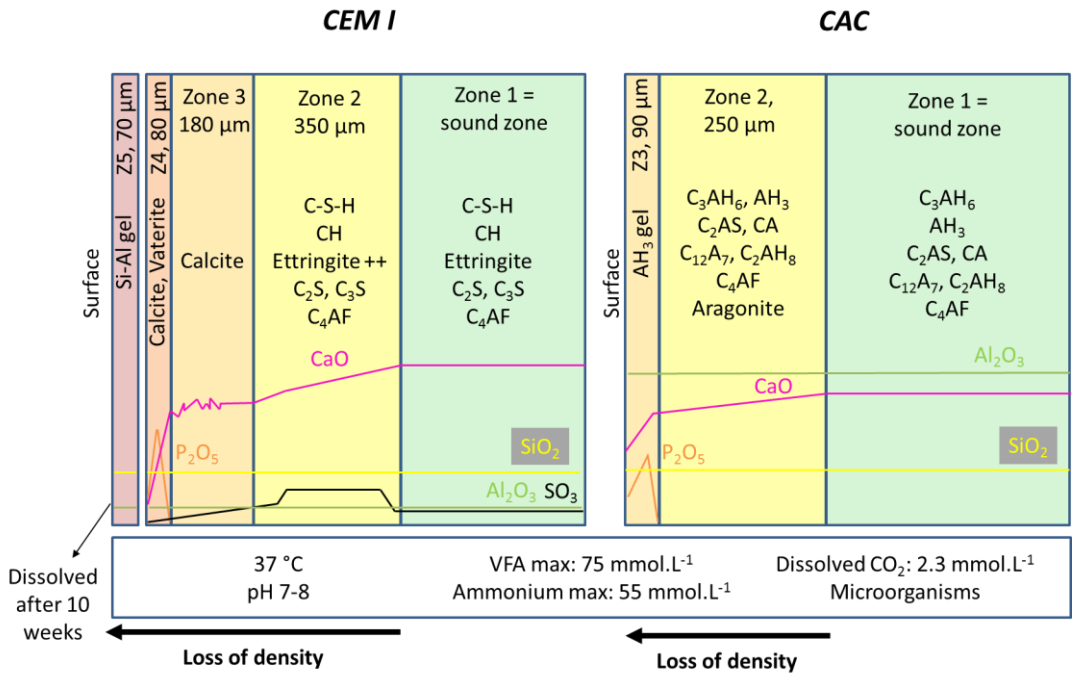

Figure 11. Chemical and mineralogical changes and degraded depths of CEM I and CAC pastes exposed to the liquid-solid phase of an anaerobic digestion bioreactor after 10 weeks of immersion and their conditions of exposure.

4.3.1 CEM I paste

In accordance with Voegel et al. [7], the analyses for the ordinary Portland cement showed alteration mechanisms corresponding to a combination of (i) leaching resulting from the exposure of cementitious materials to VFA [62] and ammonium [20], and (ii) carbonation due to the presence of aqueous CO_2 [21]. As the biowaste contained little or no sulfur, it is likely that the relative enrichment in sulfur at depth, expressed by the formation of secondary non-expansive ettringite, was due to the movement of sulfur from the outer layer, where S-bearing phases were dissolved, into zone 2. The peak of phosphorus in zone 4 was associated with the presence of phosphorus in the substrate [7]. Unlike the CAC paste, the CEM I paste was significantly affected by biofilm formation, leading to an external zone that was totally decalcified: anhydrous grains were completely dissolved after only 5 weeks of immersion, from zone 5 to zone 3.

4.3.2 CAC paste

In contact with biowaste, the CAC paste underwent chemical and mineralogical changes. Several phenomena were identified, such as surface decalcification, (incomplete) dissolution of the anhydrous grains and the hydrates on the surface, precipitation of calcium carbonates at depth and a phosphorous peak in the intermediate zone. It could also be noted that the peripheral zone maintained a relatively high density. The fact that the CAC paste performs best could be linked to lower colonization of the CAC pastes compared to other binders [63,64]. Herisson et al. [65] explained this by the bacteriostatic effect of aluminium, present in large amounts in the CAC cements. It should be noted that, when considering very aggressive sulfur oxidizing conditions comparable to those in sewer networks, Buvignier et al. [61] showed no direct effect of the aluminium on the bacteria responsible for the acid attack, which the authors attributed to the adaptation of the microbial biofilm to high Al concentrations. The particular effect of CAC on microbial biofilm development was also observed in different conditions by Peyre Lavigne et al. [66] (sulfur-oxidizing biofilms) and Dalod et al. [63] (photosynthetic biofilms). Results of both studies suggested that the biofilm development and/or activity was slown down on the CAC substrates compared to the one grown on ordinary binder based materials. Moreover, Peyre Lavigne et al. [66] showed that the biofilm on CAC was less dense, and drier, and with lower microbial diversity compared to biofilm grown on other binders. Moreover, according to the literature, the formation of an aluminium gel (AH_3) on the surface leads to better durability of calcium aluminate cement matrices, since this gel is known to be stable at moderately acidic pH [37].

5. CONCLUSION

In this study, cement paste specimens were exposed to the anaerobic digestion liquid phase of laboratory reactors for 10 weeks. At the end of the experiment, all the cementitious materials tested: made of CEM I (ordinary Portland cement), CAC (calcium aluminate cement) or CEM I-Ox (CEM I treated with oxalic acid) were covered by biofilm and presented biodeterioration. The pastes were affected by alteration mechanisms including leaching, carbonation and phosphorus enrichment. However, it should be noted that differences of behaviour were highlighted according to the material. The treatment with oxalic acid seemed to protect the specimen from biodeterioration by preventing the formation of biofilm during the first 5 weeks. Calcium oxalate therefore seems to have a proliferation inhibiting effect, at least in the short term. After this period, CEM I and CEM I-Ox followed the same degradation kinetics and mechanisms, with the formation of secondary non-expansive ettringite at depth. CAC paste showed the best durability performances and smallest degraded depth in the long term. Moreover, the anhydrous phases of the CAC paste were the best preserved and some of them were still present in the surface layer. This good durability could be linked to a less dense coverage by the biofilm but probably also to the CAC mineralogy and to the formation of a peripheral gel of AH_3, stable at moderately acidic pH.

6. ACKNOWLEDGEMENTS

The authors gratefully thank the PRES Université de Toulouse and the Midi-Pyrénées Region for their financial support, and IRSTEA, Antony, for the biowaste production protocol. They also wish to thank the French National Research Agency (ANR) for funding the project BIBENdOM – ANR – 16 – CE22 – 001 DS0602.

7. REFERENCES

[1] ADEME, Fiche technique : Méthanisation, (2015).

[2] Observ'ER, Le baromètre 2017 des énergies renouvelables électriques en France, 2017.

[3] H. Fehrenbach, J. Giegrich, G. Reinhardt, U. Sayer, M. Gretz, K. Lanje, J. Schmitz, Kriterien einer nachhaltigen Bioenergienutzung im globalen Ma\s sstab, UBA-Forschungsbericht. 206 (2008) 41–112.

[4] European Biogas Association (EBA), Statistical Report 2017 - Abridged version, European Biogas Association (EBA), Brussels, 2017.

[5] A. Bertron, Understanding interactions between cementitious materials and microorganisms: a key to sustainable and safe concrete structures in various contexts, Mater. Struct. 47 (2014) 1787–1806. doi:10.1617/s11527-014-0433-1.

[6] A. Bertron, M. Peyre-Lavigne, C. Patapy, B. Erable, Biodeterioration of concrete in agricultural, agro-food and biogas plants: state of the art and challenges, RILEM Tech. Lett. 2 (2017) 83–89. doi:10.21809/rilemtechlett.2017.42.

[7] C. Voegel, A. Bertron, B. Erable, Mechanisms of cementitious material deterioration in biogas digester, Sci. Total Environ. 571 (2016) 892–901. doi:10.1016/j.scitotenv.2016.07.072.

[8] A. Koenig, F. Dehn, Biogenic acid attack on concretes in biogas plants, Biosyst. Eng. 147 (2016) 226–237. doi:10.1016/j.biosystemseng.2016.03.007.

692 [9] S. Cole, J.R. Frank, Methane from Biomass: A Systems Approach,
693 Springer Netherlands, 1988.

694 [10] G.M. Evans, J.C. Furlong, Environmental Biotechnology - Theory and
695 Application, John Wiley & Sons, 2003.

696 [11] R. Kothari, A.K. Pandey, S. Kumar, V.V. Tyagi, S.K. Tyagi, Different
697 aspects of dry anaerobic digestion for bio-energy: An overview, Renew. Sustain.
698 Energy Rev. 39 (2014) 174–195. doi:10.1016/j.rser.2014.07.011.

699 [12] Y. Li, S.Y. Park, J. Zhu, Solid-state anaerobic digestion for methane
700 production from organic waste, Renew. Sustain. Energy Rev. 15 (2011) 821–826.
701 doi:10.1016/j.rser.2010.07.042.

702 [13] M.H. Gerardi, The Microbiology of Anaerobic Digesters, John Wiley &
703 Sons, 2003.

704 [14] L. Appels, J. Baeyens, J. Degrève, R. Dewil, Principles and potential of the
705 anaerobic digestion of waste-activated sludge, Prog. Energy Combust. Sci. 34
706 (2008) 755–781. doi:10.1016/j.pecs.2008.06.002.

707 [15] M. Kayhanian, Ammonia Inhibition in High-Solids Biogasification: An
708 Overview and Practical Solutions, Environ. Technol. 20 (1999) 355–365.
709 doi:10.1080/09593332008616828.

710 [16] Y. Chen, J.J. Cheng, K.S. Creamer, Inhibition of anaerobic digestion
711 process: A review, Bioresour. Technol. 99 (2008) 4044–4064.
712 doi:10.1016/j.biortech.2007.01.057.

713 [17] A. Bertron, J. Duchesne, Attack of Cementitious Materials by Organic
714 Acids in Agricultural and Agrofood Effluents, in: Perform. Cem.-Based Mater.
715 Aggress. Aqueous Environ., Springer, Dordrecht, 2013: pp. 131–173.
716 doi:10.1007/978-94-007-5413-3_6.

717 [18] A. Koenig, F. Dehn, Main considerations for the determination and
718 evaluation of the acid resistance of cementitious materials, Mater. Struct. 49
719 (2016) 1693–1703. doi:10.1617/s11527-015-0605-7.

720 [19] A. Koenig, A. Herrmann, S. Overmann, F. Dehn, Resistance of alkali-
721 activated binders to organic acid attack: Assessment of evaluation criteria and
722 damage mechanisms, Constr. Build. Mater. 151 (2017) 405–413.
723 doi:10.1016/j.conbuildmat.2017.06.117.

724 [20] G. Escadeillas, Ammonium Nitrate Attack on Cementitious Materials, in:
725 Perform. Cem.-Based Mater. Aggress. Aqueous Environ., Springer, Dordrecht,
726 2013: pp. 113–130. doi:10.1007/978-94-007-5413-3_5.

727 [21] G. Escadeillas, H. Hornain, La durabilité des bétons vis-à-vis des
728 environnements chimiquement agressifs, in: Durabilité Bétons, Presse de l'ENCP,
729 2008: pp. 613–705.

730 [22] C. Carde, G. Escadeillas, R. François, Use of ammonium nitrate solution
731 to simulate and accelerate the leaching of cement pastes due to deionized water,
732 Mag. Concr. Res. 49 (1997) 295–301.

733 [23] F.M. Lea, The action of ammonium salts on concrete, Mag. Concr. Res. 52
734 (1965) 115–116. doi:https://doi.org/10.1680/macr.1965.17.52.115.

735 [24] V. Baroghel-Bouny, B. Capra, D. Laurens, La durabilité des armatures et
736 du béton d'enrobage, in: Durabilité Bétons, Presse de l'ENCP, 2008: pp. 303–385.

737 [25] A. Morandeau, M. Thiéry, P. Dangla, Investigation of the carbonation
738 mechanism of CH and C-S-H in terms of kinetics, microstructure changes and
739 moisture properties, Cem. Concr. Res. 56 (2014) 153–170.
740 doi:10.1016/j.cemconres.2013.11.015.

741 [26] M. Thiery, Modélisation de la carbonatation atmosphérique des matériaux
742 cimentaires : Prise en compte des effets cinétiques et des modifications
743 microstructurales et hydriques, Ecole Nationale des Ponts et Chaussées, 2005.

744 [27] C. Voegel, N. Durban, A. Bertron, Y. Landon, B. Erable, Evaluation of
745 microbial proliferation on cementitious materials exposed to biogas systems,
746 Environ. Technol. (2019) 1–11. doi:10.1080/09593330.2019.1567610.

747 [28] C. Magniont, M. Coutand, A. Bertron, X. Cameleyre, C. Lafforgue, S.
748 Beaufort, G. Escadeillas, A new test method to assess the bacterial deterioration of
749 cementitious materials, Cem. Concr. Res. 41 (2011) 429–438.
750 doi:10.1016/j.cemconres.2011.01.014.

751 [29] A. Bertron, M. Coutand, X. Cameleyre, G. Escadeillas, J. Duchesne,
752 Attaques chimique et biologique des effluents agricoles et agroalimentaires sur les
753 matériaux cimentaires, Matér. Tech. 93 (2005) s.111-s.121.
754 doi:10.1051/mattech:2006010.

755 [30] AFNOR, NF EN 206. Béton - Spécification, performances, production et
756 conformité, Paris, France, 2014.

[31] AFNOR, FD P18-011. Béton - Définition et classification des environnements chimiquement agressifs - Recommandations pour la formulation des bétons, Paris, France, 2016.

[32] S. Kamali, M. Moranville, S. Leclercq, Material and environmental parameter effects on the leaching of cement pastes: Experiments and modelling, Cem. Concr. Res. 38 (2008) 575–585. doi:10.1016/j.cemconres.2007.10.009.

[33] S. Larreur-Cayol, A. Bertron, G. Escadeillas, Degradation of cement-based materials by various organic acids in agro-industrial waste-waters, Cem. Concr. Res. 41 (2011) 882–892. doi:10.1016/j.cemconres.2011.04.007.

[34] C. Voegel, A. Bertron, B. Erable, G. Escadeillas, Chemical treatment with oxalic acid to improve the durability of cement-based materials in acid environments, in: 2015: pp. 670–678.

[35] A. Bertron, Durabilité des matériaux cimentaires soumis aux acides organiques : cas particulier des effluents d'élevage, INSA Toulouse, 2004.

[36] A. Bertron, J. Duchesne, G. Escadeillas, Durability of various binders exposed to organic acids in manure, in: Montreal, 2007.

[37] H. Fryda, F. Saucier, S. Lamberet, K. Scrivener, D. Guinot, La durabilité des bétons d'aluminates de calcium, in: Durabilité Bétons, Presse de l'ENCP, 2008: pp. 767–823.

[38] K.L. Scrivener, J.-L. Cabiron, R. Letourneux, High-performance concretes from calcium aluminate cements, Cem. Concr. Res. 29 (1999) 1215–1223. doi:10.1016/S0008-8846(99)00103-9.

779 [39] A. Buvignier, C. Patapy, M. Peyre Lavigne, E. Paul, A. Bertron,
780 Resistance to biodeterioration of aluminium-rich binders in sewer network
781 environment: study of the possible bacteriostatic effect and role of phase
782 reactivity, Cem. Concr. Res. (Submitted).

783 [40] R. Letourneux, K. Scrivener, The resistance of calcium aluminate cements
784 to acid corrosion in wastewater applications, in: Mod. Concr. Mater. Bind. Addit.
785 Admix., Thomas Telford Publishing, 1999: pp. 275–283.
786 doi:10.1680/mcmbaaa.28227.0028.

787 [41] M. Matteini, Inorganic treatments for the consolidation and protection of
788 stone artefacts, Conserv. Sci. Cult. Herit. 8 (2008) 13–27. doi:10.6092/issn.1973-
789 9494/1393.

790 [42] D. Pinna, B. Salvadori, S. Porcinai, Evaluation of the application
791 conditions of artificial protection treatments on salt-laden limestones and marble,
792 Constr. Build. Mater. 25 (2011) 2723–2732.
793 doi:10.1016/j.conbuildmat.2010.12.023.

794 [43] A. Burgos-Cara, E. Ruiz-Agudo, C. Rodriguez-Navarro, Effectiveness of
795 oxalic acid treatments for the protection of marble surfaces, Mater. Des. 115
796 (2017) 82–92. doi:10.1016/j.matdes.2016.11.037.

797 [44] E. Hansen, E. Doehne, J. Fidler, J. Larson, B. Martin, M. Matteini, C.
798 Rodriguez-Navarro, E.S. Pardo, C. Price, A. de Tagle, J.M. Teutonico, N. Weiss,
799 A review of selected inorganic consolidants and protective treatments for porous
800 calcareous materials, Stud. Conserv. 48 (2003) 13–25.
801 doi:10.1179/sic.2003.48.Supplement-1.13.

802 [45] AFNOR, NF EN 196-3. Méthodes d'essai des ciments — Partie 3 :
803 Détermination du temps de prise et de la stabilité, 2017.

804 [46] AFNOR, NF P18-459. Essai pour béton durci - Essai de porosité et de
805 masse volumique, Paris, France, 2010.

806 [47] L. Neves, R. Oliveira, M.M. Alves, Influence of inoculum activity on the
807 bio-methanization of a kitchen waste under different waste/inoculum ratios,
808 Process Biochem. 39 (2004) 2019–2024. doi:10.1016/j.procbio.2003.10.002.

809 [48] C. Voegel, A. Bertron, B. Erable, Biodeterioration of cementitious
810 materials in biogas digester, Matér. Tech. 103 (2015) 202.
811 doi:10.1051/mattech/2015023.

812 [49] P.L. McCarty, Anaerobic Waste treatment Fundamentals, Public Works.
813 95 (1964) 66.

814 [50] P. Vindis, M. Mursec, M. Janzekovic, F. Cus, The impact of mesophilic
815 and thermophilic anaerobic digestion on biogas production, J. Achiev. Mater.
816 Manuf. Eng. 36 (2009) 192–198.

817 [51] D.P. Chynoweth, Renewable Biomethane From Land and Ocean Energy
818 Crops and Organic Wastes, HortScience. 40 (2005) 283–286.
819 doi:10.21273/HORTSCI.40.2.283.

820 [52] A. Bertron, G. Escadeillas, P. de Parseval, J. Duchesne, Processing of
821 electron microprobe data from the analysis of altered cementitious materials,
822 Cem. Concr. Res. 39 (2009) 929–935. doi:10.1016/j.cemconres.2009.06.011.

[53] A. Bertron, J. Duchesne, G. Escadeillas, Accelerated tests of hardened cement pastes alteration by organic acids: analysis of the pH effect, Cem. Concr. Res. 35 (2005) 155–166. doi:10.1016/j.cemconres.2004.09.009.

[54] M. Giroudon, M. Peyre-Lavigne, C. Patapy, A. Bertron, Biodeterioration mechanisms and kinetics of SCM and aluminate based cements and AAM in the liquid phase of anaerobic digestion, MATEC Web Conf. 199 (2018) 02003. doi:10.1051/matecconf/201819902003.

[55] P. Faucon, F. Adenot, J.F. Jacquinot, J.C. Petit, R. Cabrillac, M. Jorda, Long-term behaviour of cement pastes used for nuclear waste disposal: review of physico-chemical mechanisms of water degradation, Cem. Concr. Res. 28 (1998) 847–857. doi:10.1016/S0008-8846(98)00053-2.

[56] L. Black, C. Breen, J. Yarwood, Structural Features of C–S–H(I) and Its Carbonation in Air—A Raman Spectroscopic Study. Part II: Carbonated Phases, J. Am. Ceram. Soc. 3 (2007) 908–917.

[57] S. Goñi, A. Guerrero, Accelerated carbonation of Friedel's salt in calcium aluminate cement paste, Cem. Concr. Res. 33 (2003) 21–26. doi:10.1016/S0008-8846(02)00910-9.

[58] D. Karakashev, D.J. Batstone, I. Angelidaki, Influence of Environmental Conditions on Methanogenic Compositions in Anaerobic Biogas Reactors, Appl. Environ. Microbiol. 71 (2005) 331–338. doi:10.1128/AEM.71.1.331-338.2005.

[59] O. Yenigün, B. Demirel, Ammonia inhibition in anaerobic digestion: A review, Process Biochem. 48 (2013) 901–911. doi:10.1016/j.procbio.2013.04.012.

[60] S.R. Jenkins, J.M. Morgan, C.L. Sawyer, Measuring Anaerobic Sludge Digestion and Growth by a Simple Alkalimetric Titration, J. Water Pollut. Control Fed. 55 (1983) 448–453.

[61] A. Buvignier, M. Peyre-Lavigne, C. Patapy, E. Paul, A. Bertron, Understanding the resistance of calcium aluminate cements in sewer environments: role of soluble aluminium on the SOB activity, in: Ghent University, Belgium, 2017: pp. 215–216.

[62] A. Bertron, J. Duchesne, G. Escadeillas, Degradation of cement pastes by organic acids, Mater. Struct. 40 (2007) 341–354. doi:10.1617/s11527-006-9110-3.

[63] E. Dalod, A. Govin, R. Guyonnet, P. Grosseau, C. Lors, D. Damidot, Influence of the chemical composition of mortars on algal biofouling, in: K.L. Fentiman C.H.;.Mangabhai, R.J.;.Scrivener (Ed.), Int. Conf. Calcium Aluminates, IHS BRE Press, Palais des Papes, Avignon, France, 2014: pp. 523–534.

[64] A. Govin, I. Albuquerque, P. Grosseau, Development of an accelerated test of fungal biodeterioration. Application to calcium aluminate cements, in: K.L. Fentiman C.H.;.Mangabhai, R.J.;.Scrivener (Ed.), Int. Conf. Calcium Aluminates, IHS BRE Press, Palais des Papes, Avignon, France, 2014: pp. 511–522.

[65] J. Herisson, M. Guéguen-Minerbe, E.D. van Hullebusch, T. Chaussadent, Behaviour of different cementitious material formulations in sewer networks, Water Sci. Technol. 69 (2014) 1502–1508. doi:10.2166/wst.2014.009.

[66] M. Peyre Lavigne, A. Bertron, L. Auer, G. Hernandez-Raquet, J.-N. Foussard, G. Escadeillas, A. Cockx, E. Paul, An innovative approach to reproduce

867 the biodeterioration of industrial cementitious products in a sewer environment.
868 Part I: Test design, Cem. Concr. Res. 73 (2015) 246–256.
869 doi:10.1016/j.cemconres.2014.10.025.
870